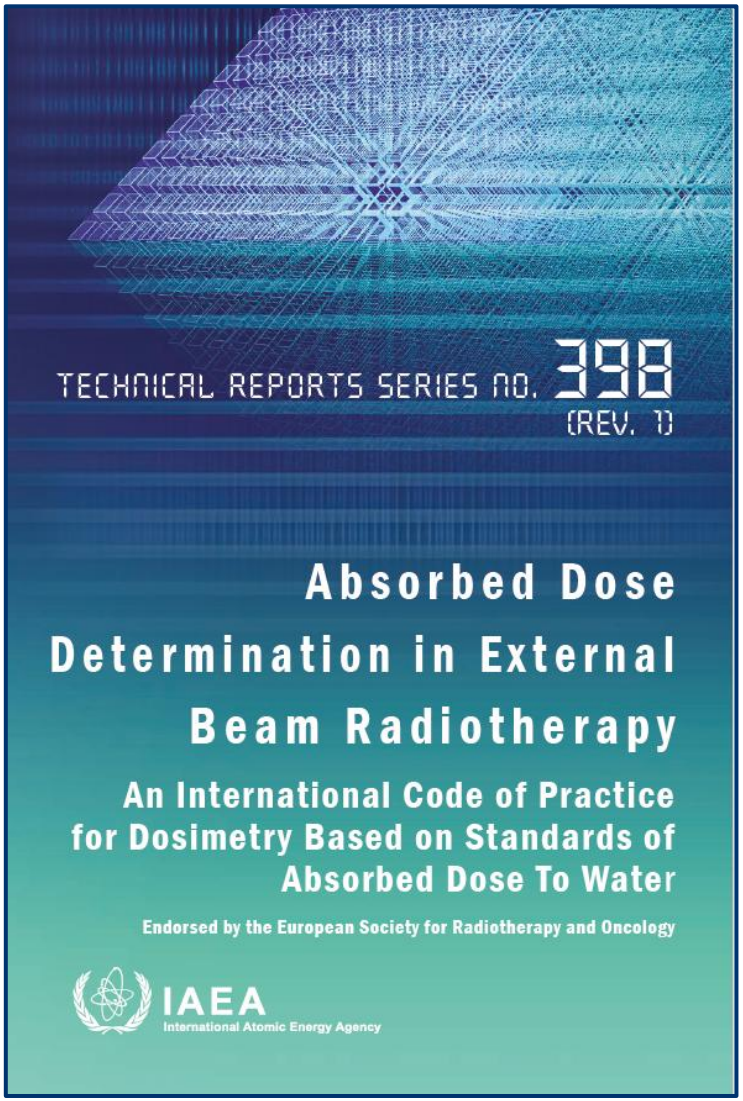

IAEA TRS-398 Rev. 1 – Intro and COP for proton and ion beams

Hugo Palmans

National Physical Laboratory, Teddington, UK and MedAustron, Wiener Neustadt, Austria

Average energy loss – stopping power - Bragg peak

Bethe-equation for mass electronic stopping power

Non-relativistic: $\frac{S_{el}}{\rho} = -\frac{dE_p}{\rho dx} = \frac{4\pi\, e^4}{(4\pi\,\varepsilon_0)^2 m_e {v_p}^2} \frac{Zz^2}{uA} \ln\left(\frac{m_e {v_p}^2}{I}\right)$

Relativistic: $\frac{S_{el}}{\rho} = \frac{4\pi {r_e}^2 m_e c^2}{\beta^2} \frac{Zz^2}{uA} \left[\frac{1}{2} ln\left(\frac{2m_e c^2 \beta^2 W_m}{1-\beta^2}\right) - \beta^2 - ln(I)\right]$

$\sim \frac{1}{{v_p}^2}$ to first order

Average energy loss – stopping power - Bragg peak

Bethe-equation for mass electronic stopping power

Non-relativistic: $\frac{S_{el}}{\rho} = -\frac{dE_p}{\rho dx} = \frac{4\pi e^4}{(} \frac{Zz^2}{} \ln\left(\frac{m_e {v_p}^2}{}\right)$

Relativistic: $\frac{S_{el}}{\rho} = \frac{4\pi {r_e}^2 m_e c^2}{\beta^2} \frac{Zz^2}{uA} \left[\frac{1}{2}\right.$

$\sim \frac{1}{{v_p}^2}$ to first order

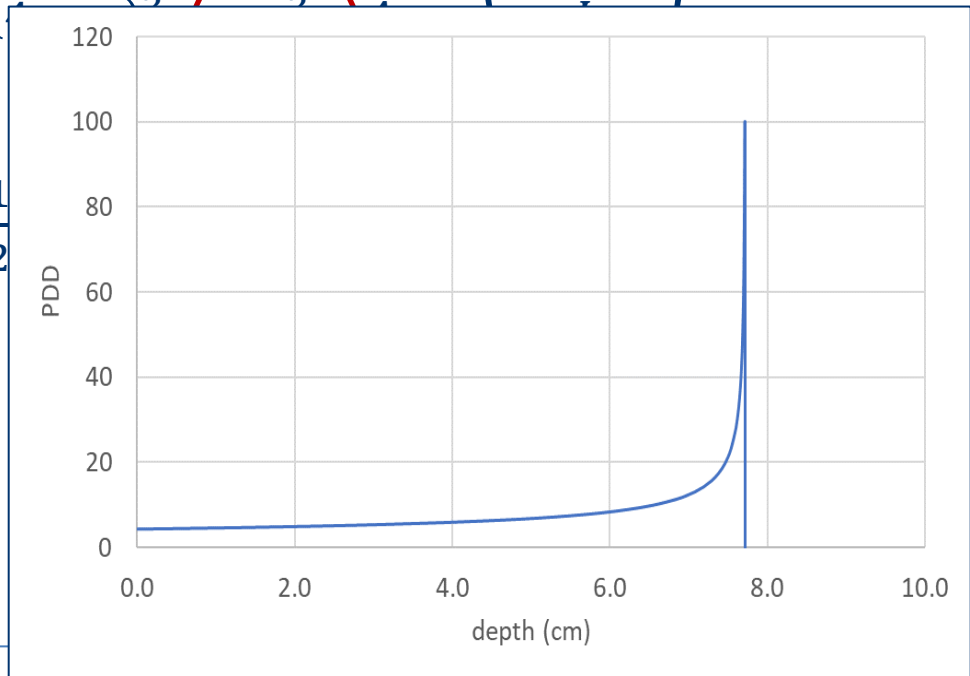

Average energy loss – stopping power - Bragg peak

Bethe-equation for mass electronic stopping power

Non-relativistic: $\frac{S_{el}}{\rho} = -\frac{dE_p}{\rho dx} = \frac{4\pi e^4}{(} \frac{Zz^2}{} \ln\left(\frac{m_e {v_p}^2}{}\right)$

Relativistic: $\frac{S_{el}}{\rho} = \frac{4\pi {r_e}^2 m_e c^2}{\beta^2} \frac{Zz^2}{uA} \left[\frac{1}{2}\right.$

$\sim \frac{1}{{v_p}^2}$ to first order

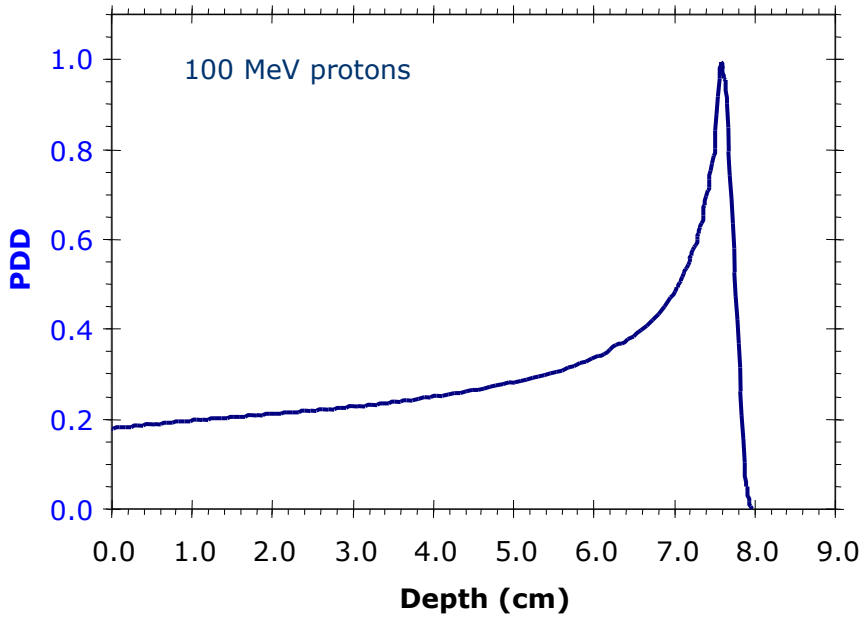

Proton beams: Spread-out Bragg peak (SOBP)

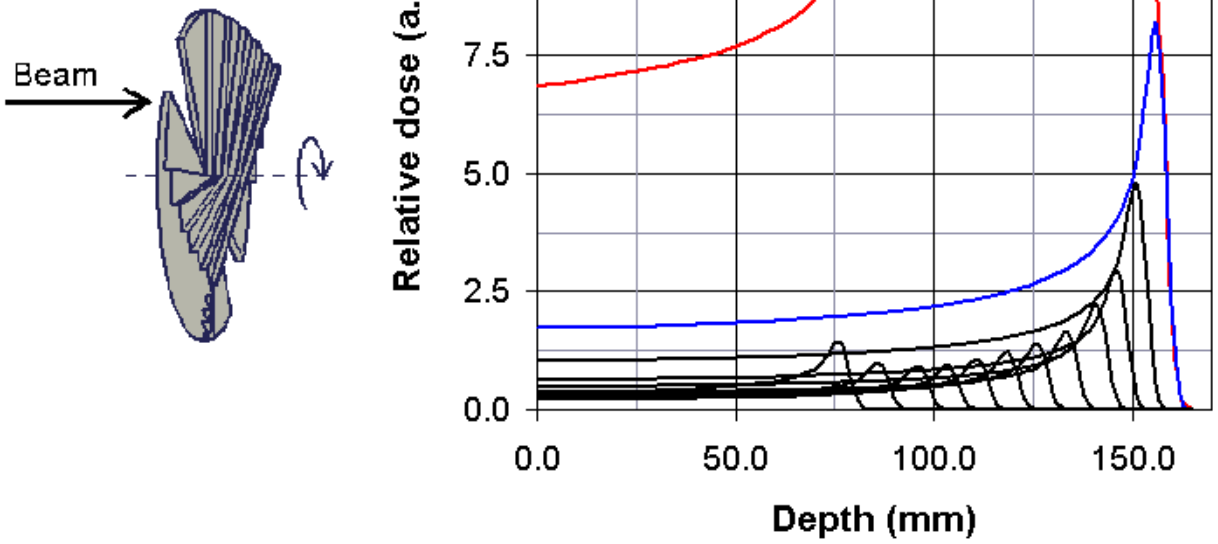

Proton beams: Spread-out Bragg peak (SOBP)

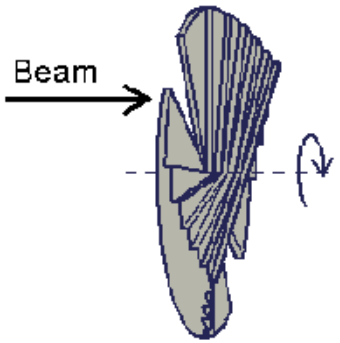

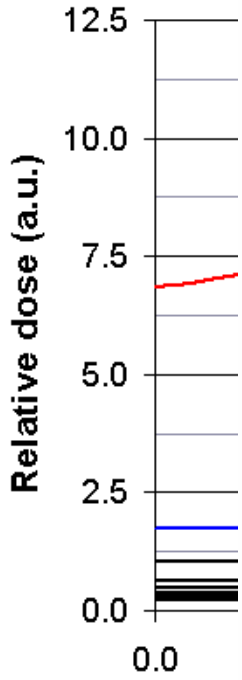

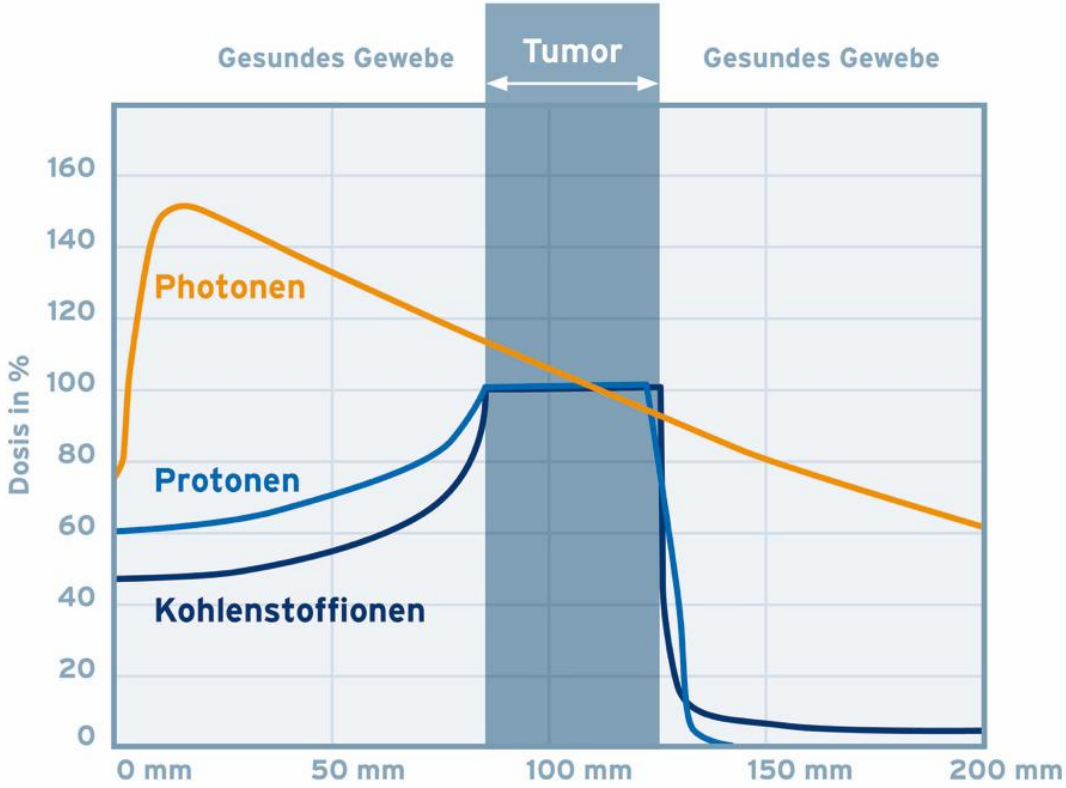

Acceleration - cyclotron

- Constant magnetic field
- Constant frequency

$$\omega = \frac{v}{\rho} = \frac{vqB}{mv} = \frac{qB}{m}$$

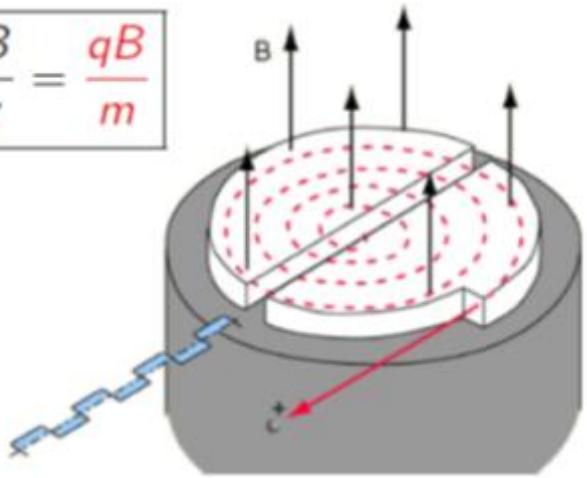

- Spiral trajectory, i.e. ρ is variable
- Constant acceleration frequency
- Synchronization of acceleration is only possible for low energies $\gamma \sim 1$ (Protons < 20 MeV), due to the relativistic mass increase:

Solutions:

* Synchro-cyclotron: modulation of the RF frequency (only pulsed operation)
* Isochroneous cyclotron: modulation of the magnetic field + hills and valleys for focussing

Acceleration - synchrotron

- Particles follow a circular orbit of constant radius inside a vacuum chamber in the form of a donut.
- Donut is placed into a magnetic field that changes in time to account for the particle mass increase with energy.

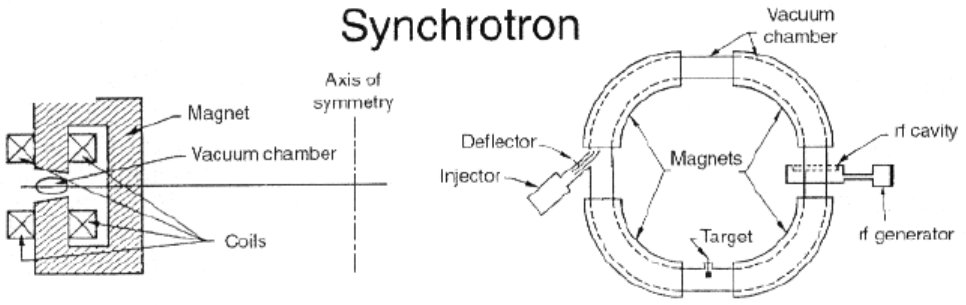

- Particles are accelerated by an RF electric field which is localized at a certain point of the vacuum chamber and is obtained by exiting stationary electromagnetic waves in a resonance cavity through which particles pass.

Acceleration - synchrotron

- Particles follow a circular orbit o
  vacuum chamber in the form of
- Donut is placed into a magnetic
  to account for the particle mass

Synchrotr

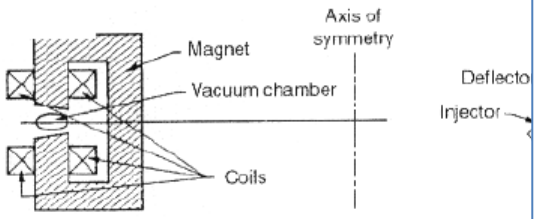

- Particles are accelerated by an R
  localized at a certain point of the
  obtained by exiting stationary el
  resonance cavity through which

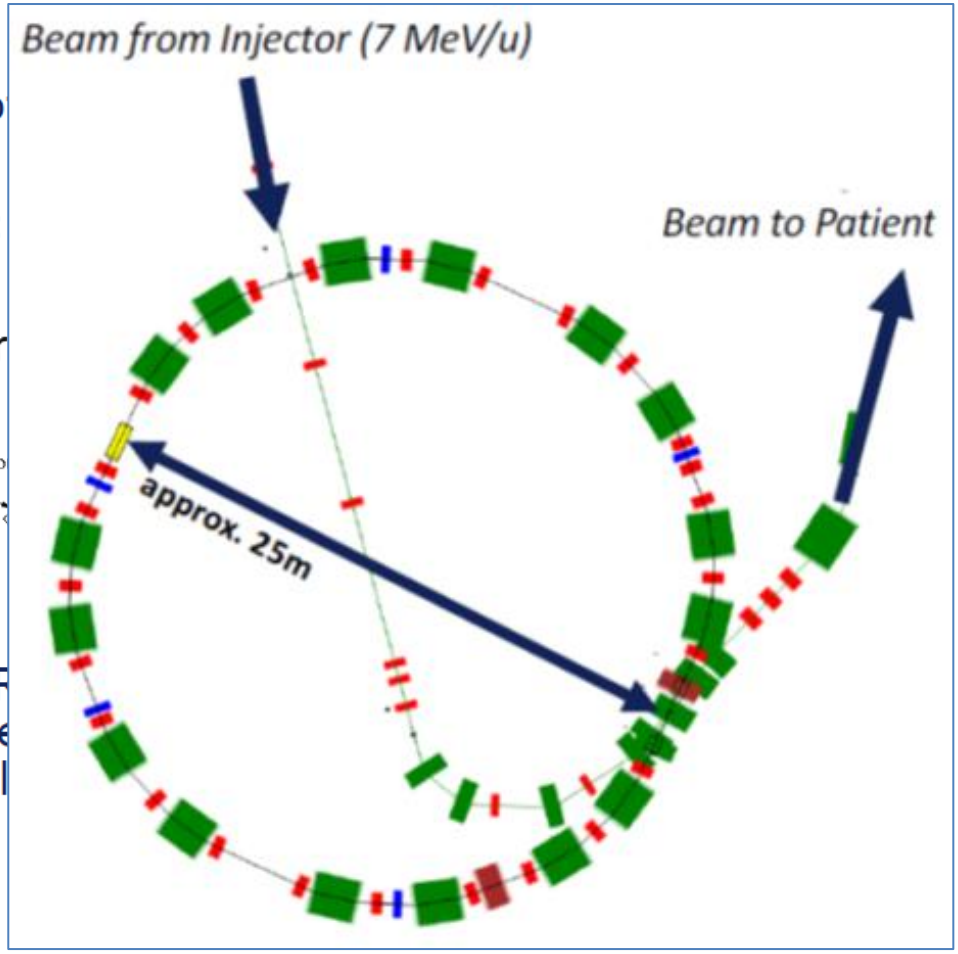

Beam delivery – passive scattering versus scanning

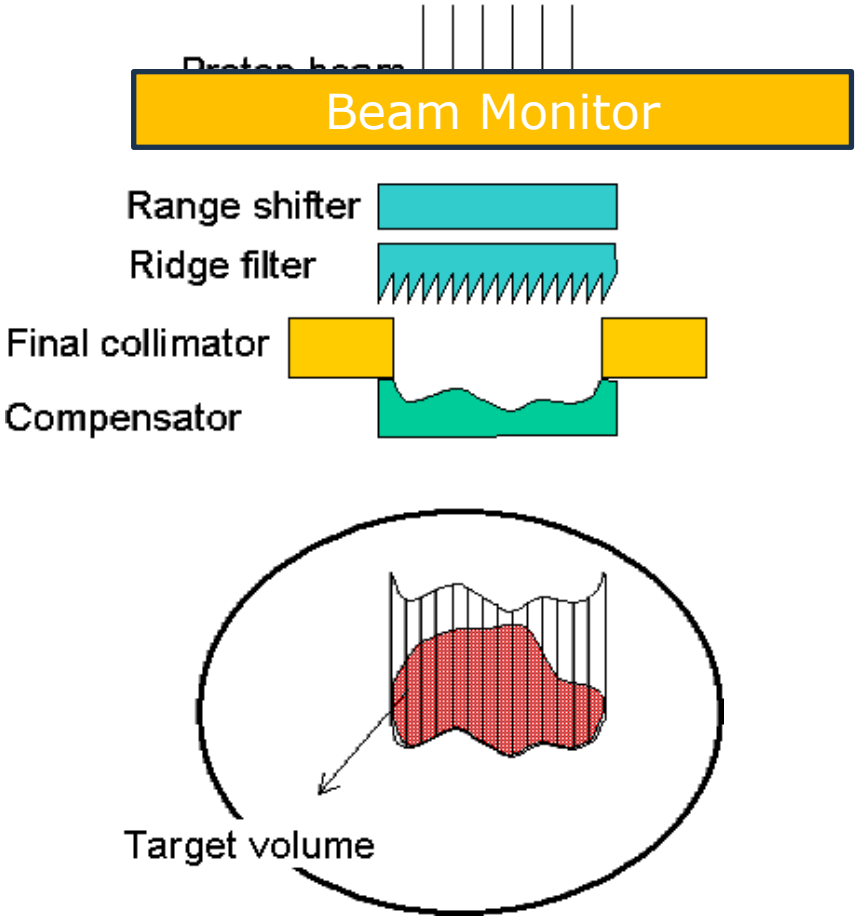

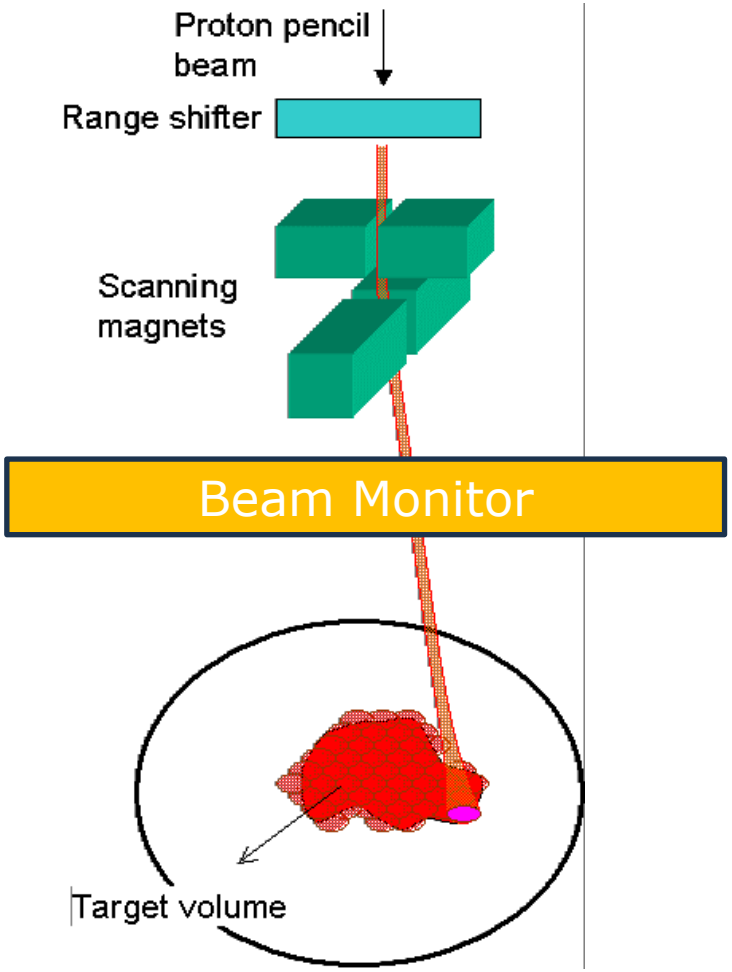

Reference conditions

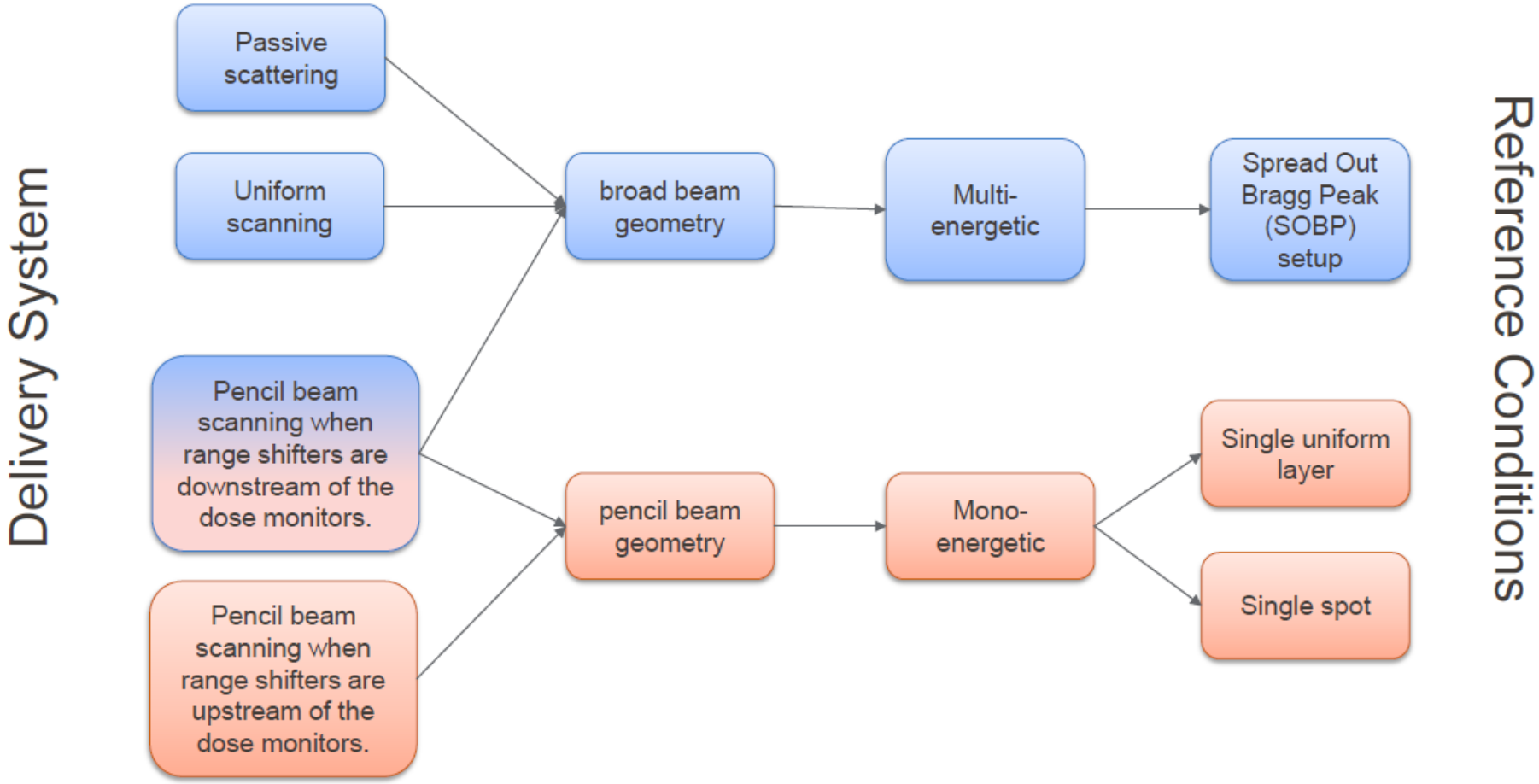

10 - CODE OF PRACTICE FOR PROTON BEAMS

1. General
2. Dosimetry equipment
   - Ionization chambers
   - Phantoms and chamber sleeves
3. Beam quality specification
   - Choice of beam quality index
   - Measurement of beam quality
4. Determination of absorbed dose to water
   - Reference conditions
   - Determination of D_w under reference conditions
   - Recombination correction
5. Values for k_{Q,Q_0}
6. Cross calibration of field ionization chambers
7. Measurements under non-reference conditions
   - Central-axis depth-dose distributions
   - Field output factors
   - Use of plastic phantoms
8. Estimated uncertainty in D_w under reference conditions
9. Worksheet

TRS-398 Rev. 1

Core group:

Pedro Andreo
David Burns
Malcolm McEwen
Brendan Healy
Ralph-Peter Kapsch
Stanislav Vatnitsky
Karen Christaki / Mauro Carrara

Working group Electrons

WG Chair: Malcolm McEwe

Rúben Dias
Mahrez
Foden
De Bruyne
Fernandinh

Working group HE photons

WG Chair: Ralph-Peter Kapsch

Marquinhos
Navas
Verratti
Florenzi
Kimpembe

Working group Lions

WG co-chairs: Stanislav Vatnitsky & Hugo Palmans

Joakim Medin
Stefaan Vynckier
Nobu Kanematsu
Oliver Jaekel

How does this look like for proton beams

Formalism: $D_{\mathrm{w},Q} = M_Q N_{D,\mathrm{w}} k_Q$

Beam quality index is R_{res}

Reference conditions for R_{res} and D_w determination + uncertainty

Cross calibration of field ionization chamber

P_{eff} shift for PDDs!

Equipment – ionization chambers

Farmer Chamber
- 30013
- waterproof
- 0.6cc
- 3.05 mm radius
- 23.0 mm length
- Gold standard for absorbed dose measurements

Advanced Markus
- 34045
- parallel plane chamber
- 5 mm dia. active area
- 2 mm guard ring
- Mainstay of electron dosimetry

PinPoint 3D ion chamber
- 31022
- Waterproof
- 0.016 cc
- 1.45 mm radius
- 2.9 mm length
- Acceptable for absorbed dose measurements

Equipment – ionization chambers

Farmer Chamber
- 30013
- waterproof
- 0.6cc
- 3.05 mm radius
- 23.0 mm length
- Gold standard for absc

PinPoint 3D ion chamber
- 31022
- Waterproof
- 0.016 cc
- 1.45 mm radius
- 2.9 mm length
- Acceptable for absorb

Bragg peak chamber
- 34080 or 34070
- parallel plane chamber
- 81.6 mm dia. active area
- Window WET: 0.7mm or 4 mm
- Used for depth dose measurements
- With caution calibrations using single mono-energetic pencil beams

tus

he chamber
ctive area
ring
electron dosimetry

Phantoms, sleeves

Similar as ^{60}Co, high-energy photons, electrons

Beam quality at measurement depth z = residual range

$$R_{\mathrm{res}} = R_{\mathrm{p}} - z$$

with R_p = practical range

Beam quality = residual range for single-energy beams:

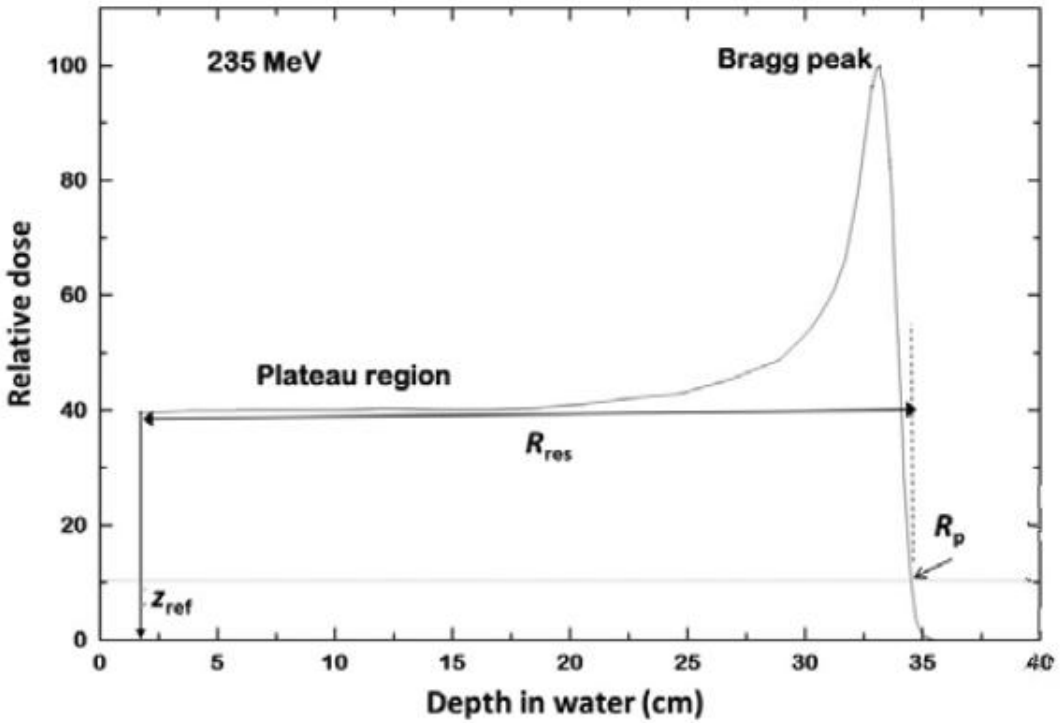

FIG. 19. Percentage depth dose distribution for a 235 MeV pristine proton beam, illustrating the plateau region and the Bragg peak. Indicated on the figure are the reference depth, z_{ref} (plateau), the residual range at z_{ref} used to specify the quality of the beam, R_{res}, and the practical range, R_p.

Beam quality = residual range for SOBP:

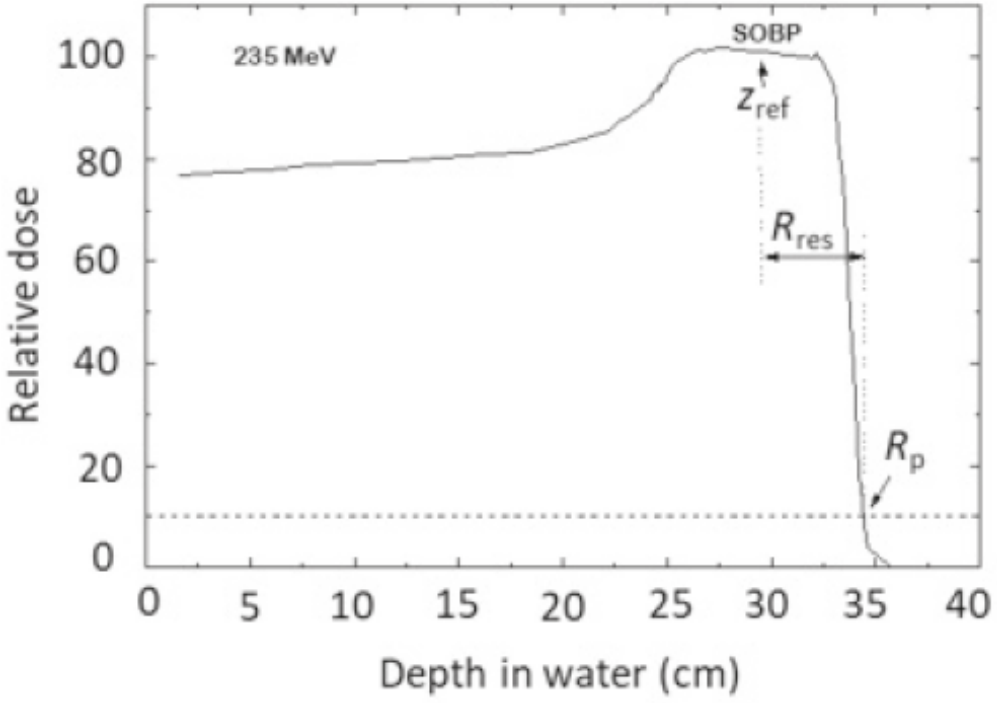

FIG. 20. Percentage depth dose distribution for a modulated proton beam. Indicated on the figure are the reference depth, z_{ref} (middle of the spread-out Bragg peak (SOBP)), the residual range at z_{ref} used to specify the quality of the beam, R_{res}, and the practical range, R_p.

Reference conditions for beam quality determination

TABLE 34. REFERENCE CONDITIONS FOR THE DETERMINATION OF PROTON BEAM QUALITY, R_{res}

Influence quantity	Reference value or reference characteristic
Phantom material	Water
Chamber type	Plane parallel
Reference point of the chamber	On the inner surface of the window at its centre
Position of the reference point of the chamber	At the point of interest
Source–surface distance	Clinical treatment distance
Field size at the phantom surface	For broad beams, 10 cm × 10 cm For small field applications (i.e. eye treatments), 10 cm × 10 cm or the largest field clinically available For scanned beams, the spot size of a single energy static pencil beam

Reference conditions for D_w (original TRS-398)

TABLE 10.II. REFERENCE CONDITIONS FOR THE DETERMINATION OF ABSORBED DOSE IN PROTON BEAMS

Influence quantity	Reference value or reference characteristics
Phantom material	water
Chamber type	for $R_{res} \geq 0.5$ g cm^{-2}, cylindrical and plane-parallel. for $R_{res} < 0.5$ g cm^{-2}, plane-parallel.
Measurement depth z_{ref}	middle of the SOBP [a]
Reference point of chamber	for plane-parallel chambers, on the inner surface of the window at its centre. For cylindrical chambers, on the central axis at the centre of the cavity volume
Position of reference point of chamber	for plane-parallel and cylindrical chambers, at the measurement depth z_{ref}.
SSD	clinical treatment distance
Field size at the phantom surface	10 cm x 10 cm, or that used for normalization of the output factors whichever is larger. For small field applications (i.e. eye treatments), 10 cm x 10 cm or the largest field clinically available

[a] The reference depth can be chosen in the "plateau region", at a depth of 3 g cm^{-2}, for clinical applications with a mono-energetic proton beam (e.g. for plateau irradiations).

Reference conditions for D_w (TRS-398 Rev.1)

TABLE 35. REFERENCE CONDITIONS FOR THE DETERMINATION OF ABSORBED DOSE TO WATER IN BROAD PROTON BEAMS CALIBRATED IN A SPREAD-OUT BRAGG PEAK

Influence quantity	Reference value or reference characteristic
Phantom material	Water
Chamber type	For $R_{res} > 0.5$ g/cm^2, cylindrical and plane parallel For $R_{res} < 0.5$ g/cm^2, plane parallel
Measurement depth, z_{ref}	Middle of the spread out Bragg peak
Reference point of the chamber	For plane parallel chambers, on the inner surface of the window, at its centre For cylindrical chambers, on the central axis, at the centre of the cavity volume
Position of the reference point of the chamber	For plane parallel and cylindrical chambers, at the measurement depth z_{ref}
Source–surface distance	Clinical treatment distance
Field size at the phantom surface	10 cm × 10 cm, or the size used for the normalization of the field output factors, whichever is larger For small field applications (i.e. eye treatments), 10 cm × 10 cm or the largest field clinically available

TABLE 36. REFERENCE CONDITIONS FOR THE DETERMINATION OF ABSORBED DOSE TO WATER IN SCANNED PROTON BEAMS CALIBRATED IN A SINGLE ENERGY PENCIL BEAM USING A SINGLE ENERGY LAYER SCANNED FIELD

Influence quantity	Reference value or reference characteristic
Phantom material	Water
Chamber type	For $R_{res} \geq 15$ g/cm^2, cylindrical and plane parallel For $R_{res} < 15$ g/cm^2, plane parallel
Measurement depth, z_{ref}	The plateau region, at a depth of 2 g/cm^2, for beams with $R_p \geq 5.0$ g/cm^2 The plateau region, at a depth of 1 g/cm^2, for beams with $R_p > 5.0$ g/cm^2
Reference point of the chamber	For plane parallel chambers, on the inner surface of the window at its centre For cylindrical chambers, on the central axis at the centre of the cavity volume
Position of the reference point of the chamber	For cylindrical and plane parallel chambers, at the measurement depth z_{ref}
Source–surface distance	Clinical treatment distance
Reference field size at the phantom surface	Uniform scanned field, large enough to achieve at least 99.5% of lateral charged particle equilibrium (i.e. the field output factor changes by <0.5% for fields larger than the reference field)

Reason for cylindrical chamber limit

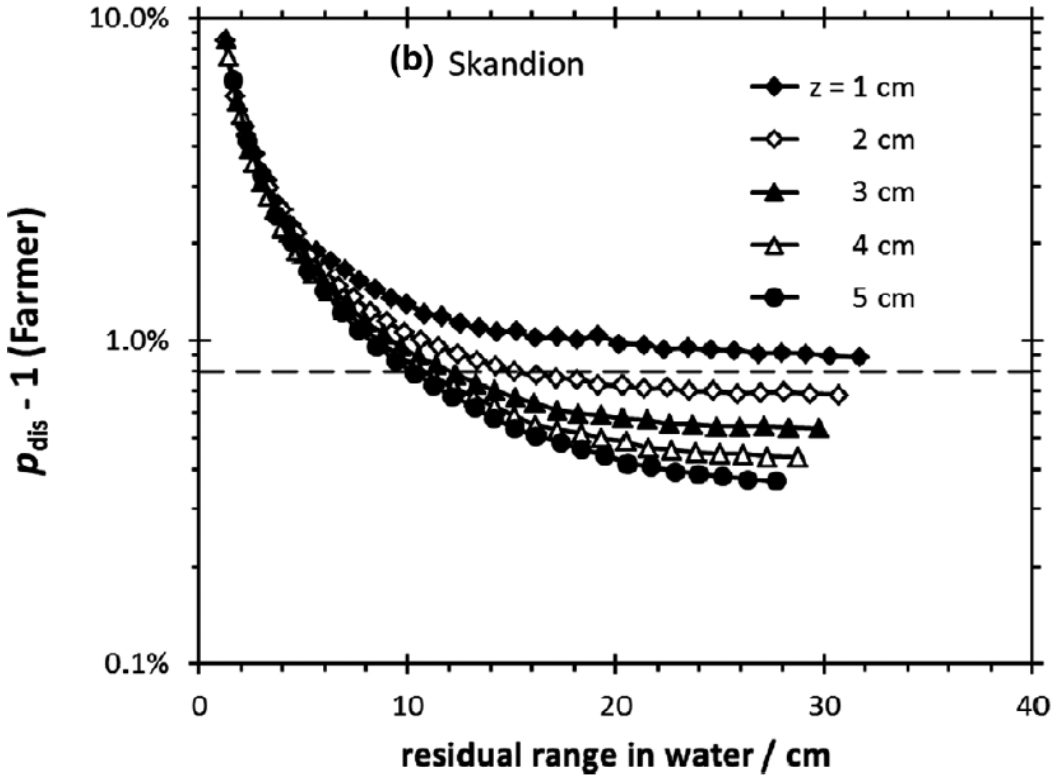

FIG 5. Displacement correction as a function of residual range for a Farmer-type ICs with a cavity diameter of 6.3 cm positioned with its center at the five measurement depths. (a) for the uncorrected MedAustron data and (b) for the Skandion data.

Palmans et al 2020
(Med Phys 47:6531)

Positioning of plane-parallel chambers

4.2.5.2. Chamber wall effects

The factor p_{wall} included in calculated k_{Q,Q_0} factors in the previous TRS-398 data corrects for the different radiation response of the chamber wall material from that of the phantom material. However, p_{wall} does not include the effect of the different attenuation of the primary fluence by the chamber wall compared with the same thickness of phantom material. When the calibration quality Q_0 and the user quality Q are the same, this attenuation is accounted for in the calibration of the chamber. Even when Q_0 is not the same as Q, the wall attenuation in photon beams is sufficiently small that cancellation may be assumed. On the other hand, in charged particle beams, the energy loss due to the chamber wall can be significantly different from that due to the same thickness of phantom material, and the water-equivalent thickness of the chamber wall should be taken into account when calculating where to position the chamber. For the chambers listed in Tables 4 and 5 the difference between physical and water-equivalent thicknesses is generally small (< 1 mm water).

Ion recombination – continuous beams

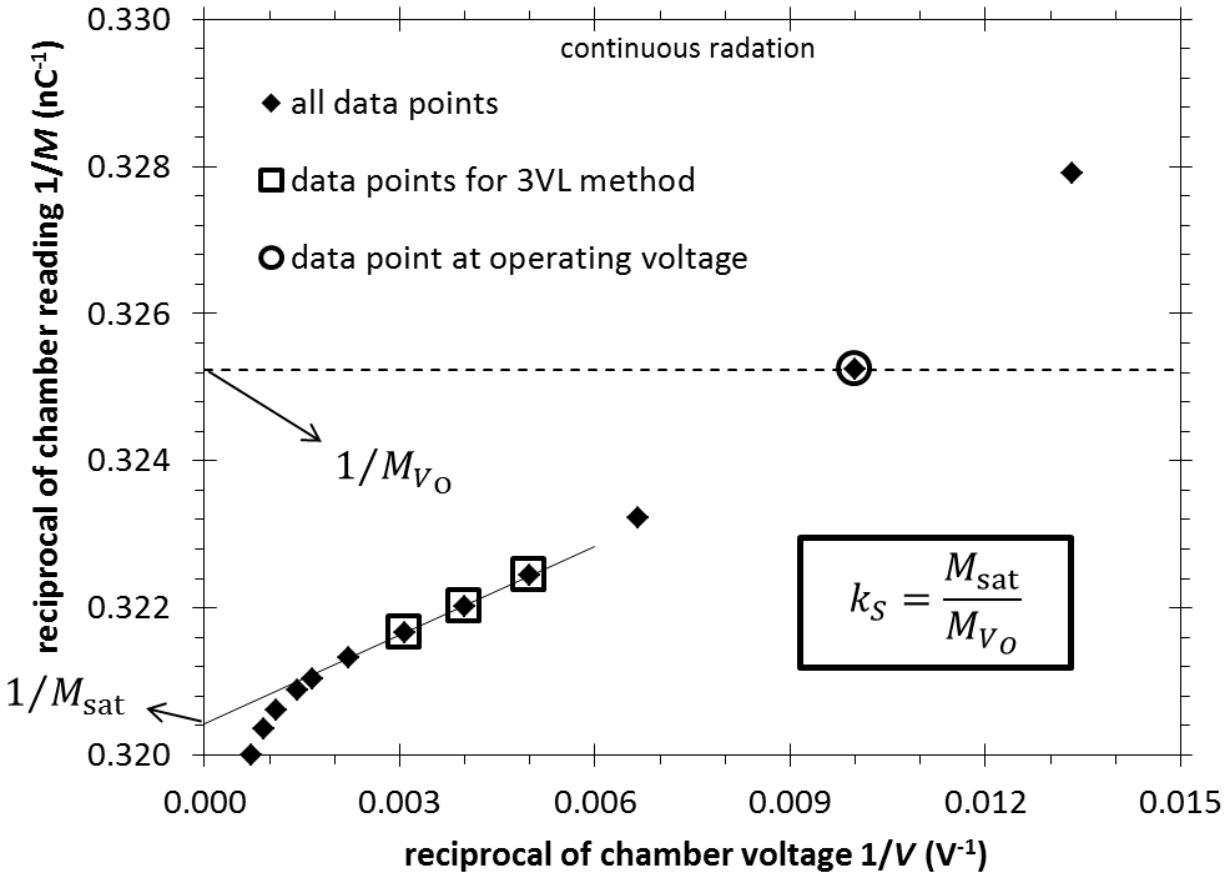

Ion recombination – pulsed beams

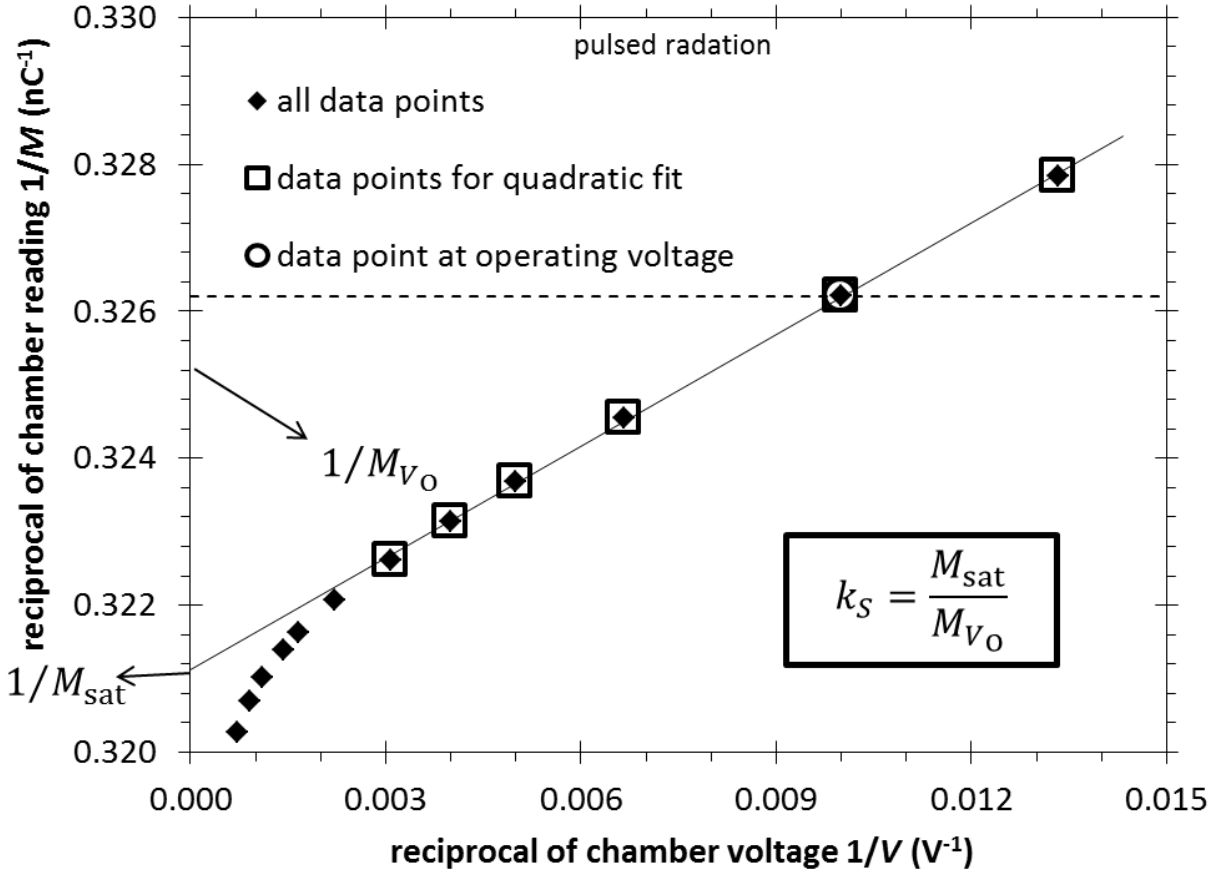

Beam quality correction factors k_Q

Collected from literature

Monte Carlo
(8 papers)

$$p_Q = \frac{(f_{ch})_Q}{(s_{w,air})_Q}$$

Experiment
(10 papers)

$$p_Q = k_Q \frac{(f_{ch})_{Q_0} (W_{air})_{Q_0}}{(s_{w,air})_Q (W_{air})_Q}$$

$$\left[k_{Q,Q_0} = \frac{(W_{air})_Q (s_{w,air})_Q p_Q}{(W_{air})_{Q_0} (s_{w,air})_{Q_0} p_{Q_0}} = \frac{(W_{air})_Q (f_{ch})_Q}{(W_{air})_{Q_0} (f_{ch})_{Q_0}} \right]$$

e.g., Farmer type chamber

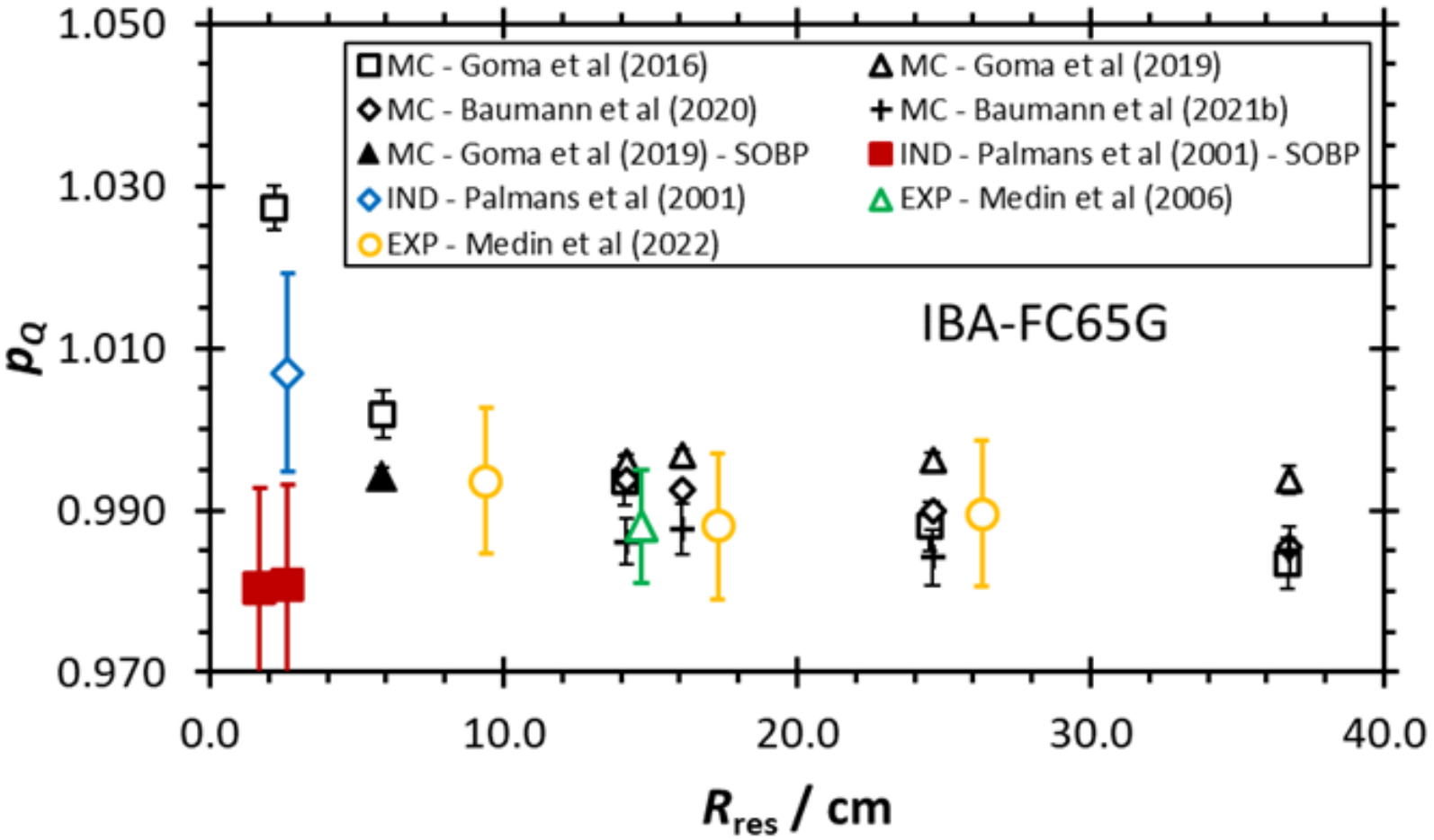

e.g., Farmer type chamber

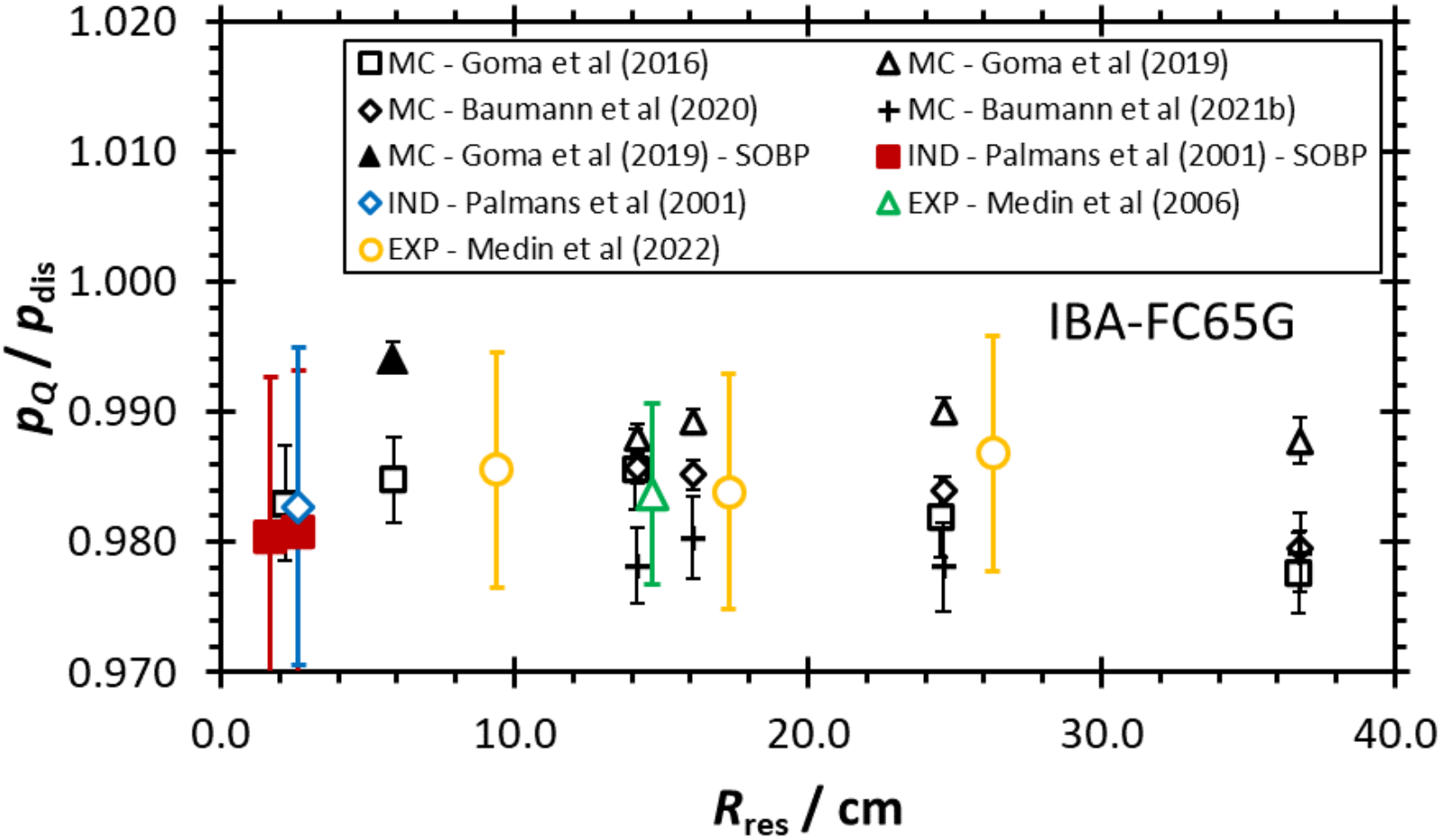

Changes compared to TRS-398

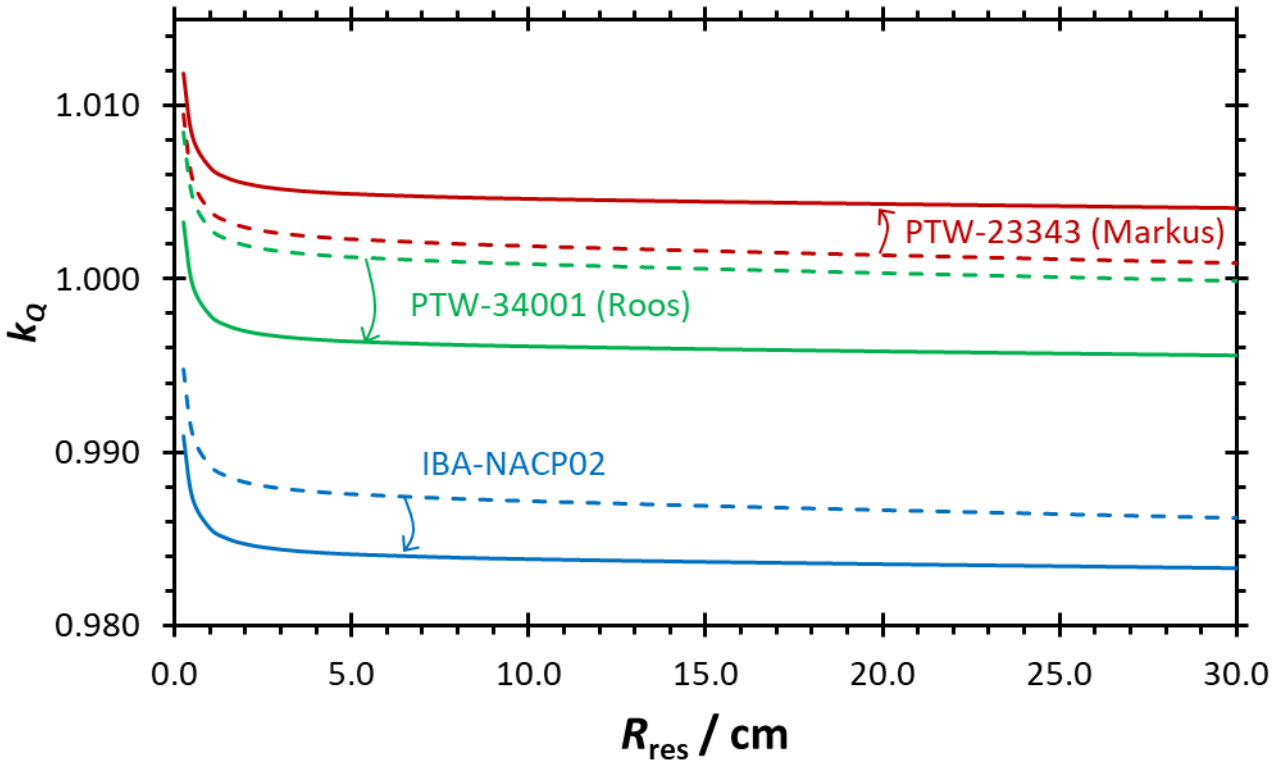

Changes compared to TRS-398

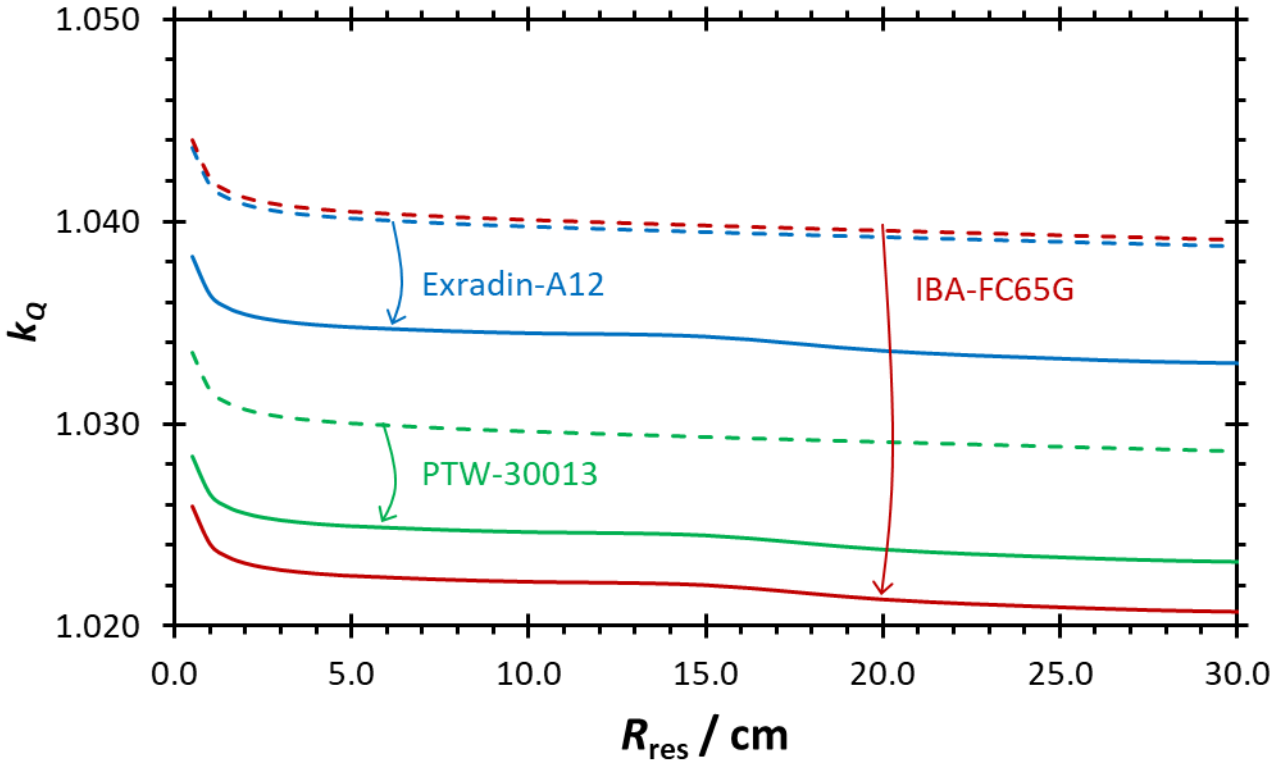

Positioning of plane-parallel chambers

4.2.5.2. Chamber wall effects

The factor p_{wall} included in calculated k_{Q,Q_0} factors in the previous TRS-398 data corrects for the different radiation response of the chamber wall material from that of the phantom material. However, p_{wall} does not include the effect of the different attenuation of the primary fluence by the chamber wall compared with the same thickness of phantom material. When the calibration quality Q_0 and the user quality Q are the same, this attenuation is accounted for in the calibration of the chamber. Even when Q_0 is not the same as Q, the wall attenuation in photon beams is sufficiently small that cancellation may be assumed. On the other hand, in charged particle beams, the energy loss due to the chamber wall can be significantly different from that due to the same thickness of phantom material, and the water-equivalent thickness of the chamber wall should be taken into account when calculating where to position the chamber. For the chambers listed in Tables 4 and 5 the difference between physical and water-equivalent thicknesses is generally small (< 1 mm water).

Difference physical thickness and WET

IOP Publishing Phys. Med. Biol. 70 (2025) 015014 https://doi.org/10.1088/1361-6560/ad9e7c

Physics in Medicine & Biology

IPEM Institute of Physics and Engineering in Medicine

PAPER

Investigating the impact of the effective point of measurement for plane-parallel ionization chambers in clinical proton beams

Kilian-Simon Baumann[1,2,3,4,*], Ana Lourenço[5,6], Jörg Wulff[7,8], Gloria Vilches-Freixas[9] and Hugo Palmans[5,10]

[1] Department of Radiotherapy and Radiooncology, University Medical Center Giessen-Marburg, Marburg, Germany
[2] University of Applied Sciences, Institute of Medical Physics and Radiation Protection, Giessen, Germany
[3] Marburg Ion-Beam Therapy Center (MIT), Marburg, Germany
[4] LOEWE Research Cluster for Advanced Medical Physics in Imaging and Therapy (ADMIT), TH Mittelhessen University of Applied Sciences, Giessen, Germany
[5] National Physical Laboratory, Teddington, United Kingdom
[6] University College London, London, United Kingdom
[7] West German Proton Therapy Centre Essen WPE, Essen, Germany
[8] University Hospital Essen, West German Cancer Center WTZ, Essen, Germany
[9] Department of Radiation Oncology (Maastro), GROW Research Institute for Oncology and Reproduction, Maastricht University Medical Centre, Maastricht, The Netherlands
[10] MedAustron Ion Therapy Center, Wiener Neustadt, Austria
[*] Author to whom any correspondence should be addressed.

E-mail: kilian-simon.baumann@staff.uni-marburg.de

Keywords: proton reference dosimetry, proton therapy, effective point of measurement, response functions, Monte Carlo, GEANT4

CrossMark

OPEN ACCESS

RECEIVED
16 August 2024

REVISED
28 November 2024

ACCEPTED FOR PUBLICATION
12 December 2024

PUBLISHED
27 December 2024

Abstract

Objective. To investigate the impact of the positioning of plane-parallel ionization chambers in proton beams on the calculation of the chamber-specific factor f_Q and, hence, the beam quality correction factor k_{Q,Q_0}. *Approach*. Monte Carlo simulations were performed to calculate the chamber-specific factor f_Q in monoenergetic proton beams for six different plane-parallel

Difference physical thickness and WET

IOP Publishing Phys. Med. Biol. 70 (2025) 015014 https://doi.org/10.1088/1361-6560/ad9e7c

Physics in Medicine & Biology IPEM

Table 1. Dimensions and materials of the entrance windows of the plane-parallel ionization chambers based on manufacturer's specifications. The mass density of each material is given in brackets. The abbreviations used are: PET for Polyethylene terephthalate, PMMA for Polyether methacrylate, and PE for Polyethylene. Additionally, the stopping power ratio (SPR) of each material in relation to water is given for 80 MeV protons calculated according to Zhang and Newhauser (2009). Furthermore, the areal mass in g cm^{-2}, the geometrical thickness in mm, the WET in mm and the shift between P_{ref} and P_{eff} is given, as well. The values for WET were calculated based on SPR as well as Monte Carlo simulations. The shift of P_{eff} relative to P_{ref} is based on Monte Carlo derived WET.

Ionization chamber	Design of entrance window	SPR material to water	Areal mass density in g cm^{-2}	Geometrical thickness in mm	WET in mm via SPR Zhang and Newhauser (2009) for 80 MeV	Monte Carlo derived WET in mm for 80 MeV	Monte Carlo derived WET in mm for 250 MeV	Shift of P_{eff} relative to P_{ref} in mm for 80 MeV	Shift of P_{eff} relative to P_{ref} in mm for 250 MeV
PTW									
Roos	1.1 mm PMMA (1.19 g cm^{-3}) 20 μm graphite (0.82 g cm^{-3})	1.165 0.734	0.133	1.120	1.30	1.30	1.36	0.18	0.24
Markus	0.87 mm PMMA (1.19 g cm^{-3}) 0.4 mm Air (1.20 mg cm^{-3}) 30 μm PE (0.93 g cm^{-3})	1.165 0.001 0.997	0.106	1.300	1.04	1.05	1.08	−0.25	−0.22
Advanced Markus	0.87 mm PMMA (1.19 g cm^{-3}) 0.4 mm Air (1.20 mg cm^{-3}) 30 μm PE (0.93 g cm^{-3})	1.165 0.001 0.997	0.106	1.300	1.04	1.05	1.07	−0.25	−0.23
IBA									
NACP-02	0.1 mm PET/Mylar (1.4 g cm^{-3}) 0.5 mm graphite (1.82 g cm^{-3})	1.311 1.630	0.105	0.600	0.95	0.95	0.98	0.35	0.38
PPC-05	0.95 mm C552 (1.76 g cm^{-3}) 50 μm graphite (1.82 g cm^{-3})	1.601 1.630	0.176	1.000	1.60	1.57	1.59	0.57	0.59
PPC-40	0.9 mm PMMA (1.19 g cm^{-3}) 0.1 mm graphite (0.93 g cm^{-3})	1.165 0.833	0.116	1.000	1.13	1.13	1.18	0.13	0.18

Difference physical thickness and WET

IOP Publishing Phys. Med. Biol. 70 (2025) 015014 https://doi.org/10.1088/1361-6560/ad9e7c

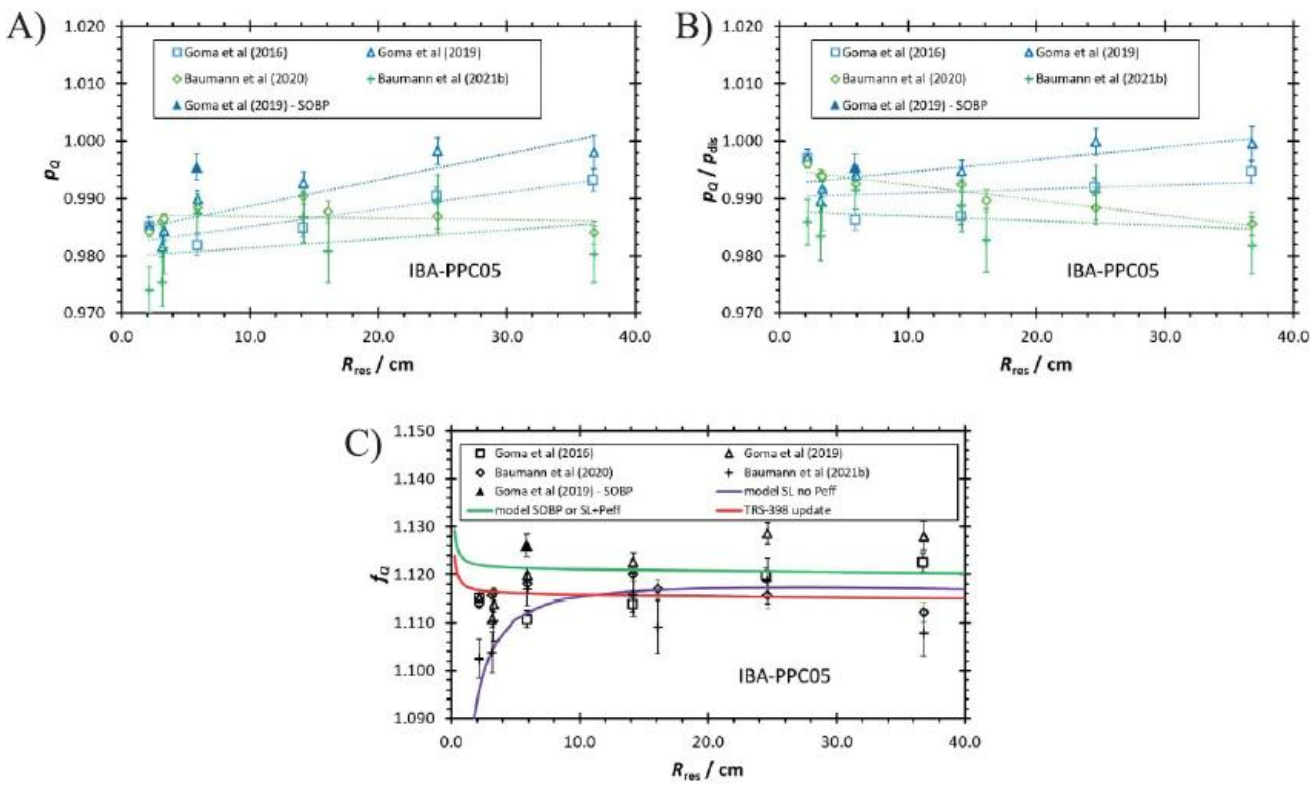

Figure 4. Average $\langle p_Q \rangle$ for the PPC-05 ionization chamber as a function of energy without (A) and with (B) accounting for displacement perturbations alongside with Monte Carlo calculated data published in the literature. In part (C) the best estimate of f_Q factors as a function of residual range for the original analysis done by Palmans *et al* (2022) in red, the new analysis from thi study in green and the approach that ionization chambers are not positioned with P_{eff} but their P_{ref} at the measurement depth in purple. SL: single layer.

Cross calibration of ionization chambers and use of a cross calibrated chamber

Similar as ^{60}Co, high-energy photons, electrons

Use of plastic phantoms strongly discouraged

the required water to plastic fluence correction factors, h_{pl}, are not well known. Nevertheless, when accurate chamber positioning in water is not possible or when no waterproof chamber is available, their use is permitted for the measurement of depth dose distributions for low energy proton beams (below ~100 MeV). In this case, the dosimeter reading at each plastic depth should be scaled using the fluence correction factor h_{pl}. It is assumed that h_{pl} has a constant value of unity at all depths.

The criteria determining the choice of plastic materials are discussed in Section 4.2.3. The density of the plastic, ρ_{pl}, should be measured for the batch in use instead of using a nominal value for the type of plastic. Each measurement depth in plastic z_{pl} (expressed in g/cm^2) also has to be scaled to give the corresponding depth in water z_w by the following equation:

$$z_w = z_{pl} c_{pl} \tag{65}$$

where c_{pl} is a depth scaling factor and z_w is expressed in units of g/cm^2. In proton dosimetry, the product $z_{pl}c_{pl}$ is commonly referred to as the water equivalent thickness of the slab. For proton beams, c_{pl} can be calculated, to a good approximation, as the ratio of the continuous slowing down approximation ranges (expressed in g/cm^2) [49] in water and in plastic. The depth scaling factor c_{pl} has a value of 0.974 for PMMA and 0.981 for clear polystyrene. The

Relative standard uncertainty on D_w

TABLE 38. ESTIMATED RELATIVE STANDARD UNCERTAINTY[a] (%) OF $D_{w,Q}$ AT THE REFERENCE DEPTH IN WATER FOR A CLINICAL PROTON BEAM BASED ON A CHAMBER CALIBRATION IN ^{60}Co GAMMA RADIATION

Physical quantity or procedure	Cylindrical and plane parallel chambers
Step 1: standards laboratory	
$N_{D,w}$ calibration of secondary standard at PSDL	0.5[b]
Long term stability of secondary standard	0.1
$N_{D,w}$ calibration of the user dosimeter at the standards laboratory	0.4
Combined uncertainty in step 1	0.6
Step 2: user proton beam	
Long term stability of user dosimeter	0.3
Establishment of reference conditions	0.4 (0.3)[c]
Dosimeter reading M_Q relative to beam monitor	0.3
Correction for influence quantities k_i	0.3
Beam quality correction, k_Q (see Appendix II)	1.4
Combined uncertainty in step 2	1.6
Combined standard uncertainty in $D_{w,Q}$ (steps 1 and 2)	1.7

11 - CODE OF PRACTICE FOR LIGHT-ION BEAMS

1. General
2. Dosimetry equipment
   - Ionization chambers
   - Phantoms and chamber sleeves
3. Beam quality specification
4. Determination of absorbed dose to water
   - Reference conditions
   - Determination of D_w under reference conditions
   - Recombination correction
5. Values for k_{Q,Q_0}
6. Measurements under non-reference conditions
7. Estimated uncertainty in D_w under reference conditions
8. Worksheet

How does this look like for carbon ions

Formalism: $D_{w,Q} = M_Q N_{D,w} k_Q$

No beam quality index

Reference conditions for D_w determination + uncertainty

Cross calibration of field ionization chamber

P_{eff} shift for reference D_w and PDDs!

Depth dose curves

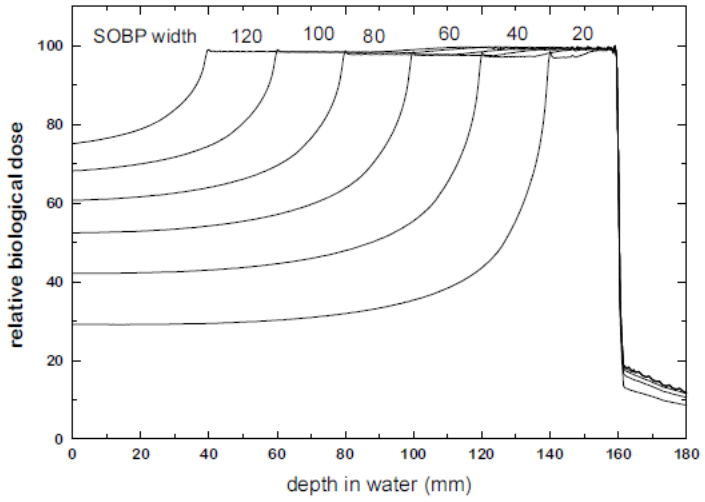

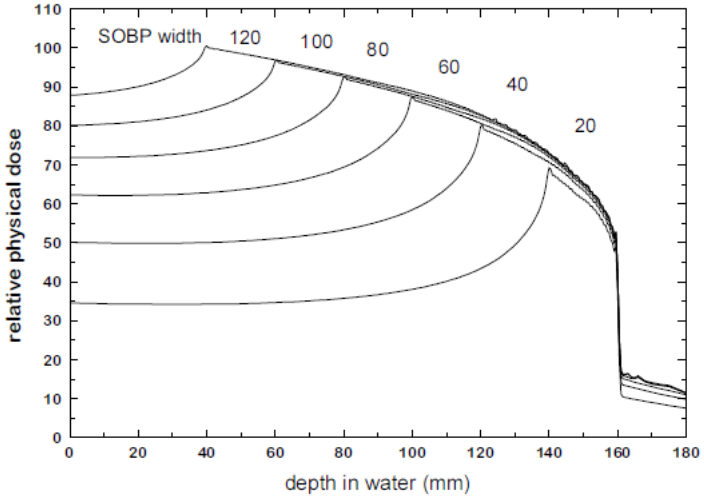

Fig. 11.2a. Biological dose distributions of therapeutic carbon beams of energy 290 MeV/u. SO mm width are designed to yield uniform biological effect in the peaks [120, 121].

Fig. 11.2b. Physical dose distributions of the beam shown in Fig 11.2(a) [120, 121].

Reference conditions for D_w

TABLE 40. REFERENCE CONDITIONS FOR THE DETERMINATION OF ABSORBED DOSE IN BROAD LIGHT ION BEAMS CALIBRATED IN THE SPREAD-OUT BRAGG PEAK

Influence quantity	Reference value or reference characteristic
Phantom material	Water
Chamber type	For SOBP width ≥2.0 g/cm^2, cylindrical and plane parallel For SOBP width <2.0 g/cm^2, plane parallel
Measurement depth, z_{ref}	Middle of the SOBP
Reference point of chamber	For plane parallel chambers, on the inner surface of the window at its centre For cylindrical chambers, on the central axis at the centre of the cavity volume
Position of reference point of chamber	For plane parallel chambers, at the measurement depth z_{ref} For cylindrical chambers, $0.75r_{cyl}$ deeper than z_{ref}
Source–surface distance	Clinical treatment distance
Field size at the phantom surface	10 cm × 10 cm, or that used for normalization of the field output factors, whichever is larger

TABLE 41. REFERENCE CONDITIONS FOR THE DETERMINATION OF ABSORBED DOSE IN SCANNED LIGHT ION BEAMS CALIBRATED IN A SINGLE ENERGY PENCIL BEAM USING A SINGLE LAYER SCANNED FIELD

Influence quantity	Reference value or reference characteristic
Phantom material	Water
Chamber type	Cylindrical and plane parallel
Measurement depth z_{ref}	The plateau region, preferentially at a depth of 1 g/cm^2 (alternatively 2 g/cm^2)
Reference point of chamber	For plane parallel chambers, on the inner surface of the window at its centre For cylindrical chambers, on the central axis at the centre of the cavity volume
Position of reference point of chamber	For plane parallel chambers, at the measurement depth z_{ref} For cylindrical chambers, $0.75r_{cyl}$ deeper than z_{ref}
Source–surface distance	Clinical treatment distance
Reference field size[a] at the phantom surface	10 cm × 10 cm or that used for normalization of the field output factors, whichever is larger

Beam quality correction factors k_Q

$$k_{Q,Q_0} = \frac{(W_{\text{air}})_Q (s_{\text{w,air}})_Q p_Q}{(W_{\text{air}})_{Q_0} (s_{\text{w,air}})_{Q_0} p_{Q_0}}$$

TABLE 42. CALCULATED VALUES OF k_Q FOR CARBON ION BEAMS[a] FOR VARIOUS CYLINDRICAL AND PLANE PARALLEL IONIZATION CHAMBERS

Ionization chamber type[b]	k_Q
Cylindrical chambers	
Capintec PR-06C Farmer	1.042
Exradin A1SL Miniature Shonka	1.043
Exradin A12 Farmer	1.040
Exradin A12S Farmer	1.042
Exradin A18	1.044
Exradin A19 Classic Farmer	1.039
Exradin A28	1.037
IBA CC13	1.027**
IBA CC25	1.030**
IBA FC23-C Short Farmer	1.030**
IBA FC65-G Farmer[c]	1.028*
IBA FC65-P Farmer	1.026**
NE 2561/2611A (NPL 2611A) Secondary Standard	1.040
NE 2571 Farmer	1.031**
PTW 30010 Farmer	1.030**
PTW 30011 Farmer	1.027**
PTW 30012 Farmer	1.037**
PTW 30013 Farmer[c]	1.028*
PTW 31010 Semiflex	1.039
PTW 31013 Semiflex	1.036
Plane parallel chambers	
Exradin A10	1.033
Exradin A11	1.035
Exradin A11TW	1.047
IBA NACP-02	0.998
IBA PPC05	0.993**
IBA PPC40	0.993**
PTW 34045 Advanced Markus	1.006
PTW 23343 Markus	1.009
PTW 34001 Roos	0.997**

Use of plastic phantoms

not mentioned

Relative standard uncertainty on D_w

TABLE 43. ESTIMATED RELATIVE STANDARD UNCERTAINTY[a] OF $D_{w,Q}$ AT THE REFERENCE DEPTH IN WATER AND FOR A CLINICAL LIGHT ION BEAM, CALIBRATED AT THE SPREAD-OUT BRAGG PEAK AND IN A SINGLE ENERGY LAYER, BASED ON A CHAMBER CALIBRATION IN ^{60}Co GAMMA RADIATION

Physical quantity or procedure	Relative standard uncertainty (%)	
	User chamber type	
	Cylindrical	Plane parallel
Step 1: standards laboratory		
$N_{D,w}$ calibration of secondary standard at a primary standards dosimetry laboratory	0.5	0.5
Long term stability of secondary standard	0.1	0.1
$N_{D,w}$ calibration of the user dosimeter at the standard laboratory	0.4	0.4
Combined uncertainty in step 1	0.6[b]	0.6[b]
Step 2: user light ion beam		
Long term stability of user dosimeter	0.2	0.4
Establishment of reference conditions	0.4 (0.6)[c]	0.6 (0.7)[c]
Dosimeter reading M_Q relative to beam monitor	0.3	0.3
Correction for influence quantities k_i	0.3	0.3
Beam quality correction, k_Q (calculated)	2.4	2.4
Combined uncertainty in step 2	2.5	2.6
Combined standard uncertainty in $D_{w,Q}$ (steps 1 and 2)	2.6	2.7